Dynamic Analysis and Reduction of a Cyclic Symmetric System Subjected to Geometric Nonlinearities

Adrien Martin, Fabrice Thouverez

Dynamic Analysis and Reduction of a Cyclic Symmetric System Subjected to Geometric Nonlinearities

Adrien Martin*, **Fabrice Thouverez**
Laboratoire de Tribologie et Dynamique des Systèmes
École Centrale de Lyon
69134 Écully CEDEX
France
Email: adrien.martin@doctorant.ec-lyon.fr

Abstract

The search for ever lighter weight has become a major goal in the aeronautical industry as it has a direct impact on fuel consumption. It also implies the design of increasingly thin structures made of sophisticated and flexible materials. This may result in nonlinear behaviours due to large structural displacements. Stator vanes can be affected by such phenomena, and as they are a critical part of turbojets, it is crucial to predict these behaviours during the design process in order to eliminate them.

This paper presents a reduced order modelling process suited for the study of geometric nonlinearities. The method is derived from a classical Component Mode Synthesis with fixed interfaces, in which the reduced nonlinear terms are obtained through a STEP procedure using an adapted basis composed of linear modes completed by modal derivatives. The whole system is solved using a harmonic balance procedure and a classic iterative nonlinear solver. The application is implemented on a schematic stator vane model composed of nonlinear Euler-Bernoulli beams under von Kàrmàn assumptions.

1 Introduction

The aim of this paper is to describe the analysis of periodic structures. They have already been studied for a long time [17] by focusing on their symmetry. The context of non-conservative nonlinearity, such as friction, is well known with the use of several vibration mitigation devices on the bladed disks. An overview of the methods used for the study of such phenomena has been proposed recently by Krack [11]. The scope of polynomial nonlinearity was considered in the 1990s by Samaranayake [15], Vakakis [19], and more recently by Georgiades [4] and Grolet [5], in the context of nonlinear normal modes (NNMs) [9], as they exhibited bifurcations in the case of simplified models composed of Duffing oscillators.

It is necessary to reduce such structures due to the size of the finite element (FE) model. Symmetry can be used to considerably reduce size by considering a reference sector and using it to determine the response of the other sectors [17]. The study proposed herein deals with a system subjected to nonlinear effects which means that the response of the structure can no longer be expressed with independent diameters, even in the case of a system with natural cyclic symmetry. However, it is possible to use classical Component Mode Synthesis (CMS) such as the Craig & Bampton [3] method and consider each sector as a substructure. Paired with NNMs, this method has been used for the study of friction nonlinearity [10, 8], and in the case of cubic nonlinearity [1].

This paper proposes an original coupling of several methods used for the study of nonlinear systems. The nonlinear effects of each substructure are reduced by using linear normal modes (LNMs) completed with modal derivatives (MD) [7, 16]. The reduced nonlinear stiffnesses associated with the basis are determined using a STiffness Evaluation Procedure (STEP) [13]. With this basis we are able to derive an original nonlinear CMS which can be used for our simluations. The originality of this work also lies in its application to a periodic structure. Indeed, the innovative approach proposed allows determining the nonlinear response of such specific structures

*Address all correspondence to this author.

within a reasonable computation time, demonstrating the improvement it provides. The model studied is a periodic stator vane modeled with nonlinear Euler-Bernoulli beams in conformity with the von Kàrmàn simplification of the Green-Lagrange tensor.

2 Reduction Procedure

The study is carried out on a n dimensional system of nonlinear equations

$$\mathbf{M}\,\ddot{\mathbf{x}}(t) + \mathbf{C}\,\dot{\mathbf{x}}(t) + \mathbf{K}\,\mathbf{x}(t) + \mathbf{f}^{\mathrm{nl}}(\mathbf{x}(t)) = \mathbf{f}^{\mathrm{ext}}(t) \tag{1}$$

where $\mathbf{x}(t)$ is the vector of unknowns, i.e. the degrees of freedom (DOFs); $\mathbf{M}$, $\mathbf{C}$ and $\mathbf{K}$ refer to the mass, damping and linear stiffness matrices; $\mathbf{f}^{\mathrm{nl}}(\mathbf{x}(t))$ describes the nonlinear forces due to the geometric effects and thus depends only on the displacements of the structure; and $\mathbf{f}^{\mathrm{ext}}(t)$ is the vector of external forces applied on the structure.

2.1 Fixed-interface Component Mode Synthesis: Craig-Bampton reduction

Let us consider the underlying linear system of Eqn. (1), written as

$$\mathbf{M}\,\ddot{\mathbf{x}}(t) + \mathbf{C}\,\dot{\mathbf{x}}(t) + \mathbf{K}\,\mathbf{x}(t) = \mathbf{f}^{\mathrm{ext}}(t) \tag{2}$$

where the nonlinear forces have been omitted.

The reduction method presented herein lies on a classical Craig-Bampton procedure [3]. Thus, the matrices are partitioned into internal ($\mathbf{x}_{\mathrm{i}}$) and boundary ($\mathbf{x}_{\mathrm{b}}$) DOFs, and the Eqn. (2) can be re-written with respect to the ordered DOFs $\mathbf{y}$

$$\begin{bmatrix} \mathbf{M}_{\mathrm{ii}} & \mathbf{M}_{\mathrm{ib}} \\ \mathbf{M}_{\mathrm{bi}} & \mathbf{M}_{\mathrm{bb}} \end{bmatrix} \ddot{\mathbf{y}}(t) + \begin{bmatrix} \mathbf{C}_{\mathrm{ii}} & \mathbf{C}_{\mathrm{ib}} \\ \mathbf{C}_{\mathrm{bi}} & \mathbf{C}_{\mathrm{bb}} \end{bmatrix} \dot{\mathbf{y}}(t) + \begin{bmatrix} \mathbf{K}_{\mathrm{ii}} & \mathbf{K}_{\mathrm{ib}} \\ \mathbf{K}_{\mathrm{bi}} & \mathbf{K}_{\mathrm{bb}} \end{bmatrix} \mathbf{y}(t) = \begin{bmatrix} \mathbf{f}_{\mathrm{i}}^{\mathrm{ext}} \\ \mathbf{f}_{\mathrm{b}}^{\mathrm{ext}} \end{bmatrix} \tag{3}$$

Each substructure is then reduced with the fixed-interface eigenvectors $\mathbf{\Phi}_{\mathrm{i}}^{j}$ associated with the internal DOFs (Eqn. (4)) and the static modes $\mathbf{\Psi}_{\mathrm{b}}^{j}$, with the coupling between the substructures obtained by successively applying a unitary displacement on one of the boundary DOF while the others are clamped (Eqn. (5)).

$$\left(\mathbf{K}_{\mathrm{ii}}^{j} - \omega^2 \mathbf{M}_{\mathrm{ii}}^{j}\right) \mathbf{\Phi}_{\mathrm{i}}^{j} = \mathbf{0} \tag{4}$$

$$\mathbf{\Psi}_{\mathrm{b}}^{j} = -\left[\mathbf{K}_{\mathrm{ii}}^{j}\right]^{-1} \mathbf{K}_{\mathrm{ib}}^{j} \tag{5}$$

The transformation from the physical coordinates $\mathbf{y}(t)$ to the reduced coordinates $\mathbf{z}(t)$ is done using matrix $\mathbf{T}_{\mathrm{CB}}$

$$\mathbf{y}(t) = \begin{bmatrix} \mathbf{x}_{\mathrm{i}}^{1}(t) \\ \vdots \\ \mathbf{x}_{\mathrm{i}}^{\mathrm{N_S}}(t) \\ \mathbf{x}_{\mathrm{b}}(t) \end{bmatrix} = \begin{bmatrix} \mathbf{\Phi}_{\mathrm{i}}^{1} & & \mathbf{\Psi}_{\mathrm{b}}^{1} \\ & \ddots & \vdots \\ & & \mathbf{\Phi}_{\mathrm{i}}^{\mathrm{N_S}} \; \mathbf{\Psi}_{\mathrm{b}}^{\mathrm{N_S}} \\ & & \mathbf{I}_{\mathrm{b}} \end{bmatrix} \begin{bmatrix} \mathbf{q}_{\mathrm{i}}^{1}(t) \\ \vdots \\ \mathbf{q}_{\mathrm{i}}^{\mathrm{N_S}}(t) \\ \mathbf{x}_{\mathrm{b}}(t) \end{bmatrix} = \mathbf{T}_{\mathrm{CB}}\,\mathbf{z}(t) \tag{6}$$

Thus, the projection of Eqn. (3) onto the subspaces spanned by $\mathbf{T}_{\mathrm{CB}}$ leads to the reduced system

$$\mathbf{M}_{\mathrm{CB}}\,\ddot{\mathbf{z}}(t) + \mathbf{C}_{\mathrm{CB}}\,\dot{\mathbf{z}}(t) + \mathbf{K}_{\mathrm{CB}}\,\mathbf{z}(t) = \mathbf{f}_{\mathrm{CB}}^{\mathrm{ext}}(t) \tag{7}$$

where $\mathbf{A}_{\mathrm{CB}} = \mathbf{T}_{\mathrm{CB}}^{\intercal}\,\mathbf{A}\,\mathbf{T}_{\mathrm{CB}}$ for the matrices, and $\mathbf{a}_{\mathrm{CB}} = \mathbf{T}_{\mathrm{CB}}^{\intercal}\,\mathbf{a}$ for the vectors.

2.2 Computation of the reduced nonlinear terms

2.2.1 Formulation and hypothesises

Two hypothesises are made to extend the CMS procedure to the nonlinear forces. The first one, already used in the context of polynomial nonlinearity [1, 14], assumes that the static modes, and thus the DOFs associated with them, remain linear. It has shown its reliability in the framework of Duffing oscillators [1, 14]. The second hypothesis assumes that the nonlinear terms depend only on the reduced coordinates associated with the internal modes. This results in expressing the reduced nonlinear forces as

$$\mathbf{f}_{\mathrm{CB}}^{\mathrm{nl}}(\mathbf{z}(t)) = \begin{bmatrix} \left[\boldsymbol{\Phi}_{\mathrm{i}}^{1}\right]^{\intercal} \mathbf{f}^{1,\mathrm{nl}}\left(\boldsymbol{\Phi}_{\mathrm{i}}^{1}\,\mathbf{q}_{\mathrm{i}}^{1}(t)\right) \\ \vdots \\ \left[\boldsymbol{\Phi}_{\mathrm{i}}^{\mathrm{N_S}}\right]^{\intercal} \mathbf{f}^{\mathrm{N_S},\mathrm{nl}}\left(\boldsymbol{\Phi}_{\mathrm{i}}^{\mathrm{N_S}}\,\mathbf{q}_{\mathrm{i}}^{\mathrm{N_S}}(t)\right) \\ \mathbf{0} \end{bmatrix} \tag{8}$$

2.2.2 Completing the internal modes: modal derivatives

The basis used for the projection of the nonlinear terms is critical for the precision of the reduction. Some of them have already been studied and used. LNMs have shown their capacities to take into account the membrane-flexion coupling [12] induced by the nonlinearities, but they require numerous vectors to do so. Regarding the procedure for projecting the nonlinear terms onto the basis presented further on, it must be kept as small as possible. Thus, the choice was made to use modal derivatives [7, 16], due to their capacities to take into account coupling effects along with LNMs. Their mathematical origin lies in the fact that NNMs depend on the amplitude of the DOFs. Using a Galerkin procedure, the solution can be developed by applying Taylor's expansion

$$\begin{aligned} \mathbf{x}(\mathbf{q}) &= \boldsymbol{\Phi}(\mathbf{q})\,\mathbf{q} \\ &= \mathbf{x}(\mathbf{q}=\mathbf{0}) + \sum_{k=1}^{\mathrm{r}} \left.\frac{\partial \mathbf{x}}{\partial \mathrm{q}_k}\right|_{\mathbf{q}=\mathbf{0}} \mathrm{q}_k + \frac{1}{2}\sum_{k,l=1}^{\mathrm{r}} \left.\frac{\partial^2 \mathbf{x}}{\partial \mathrm{q}_k \partial \mathrm{q}_l}\right|_{\mathbf{q}=\mathbf{0}} \mathrm{q}_k \mathrm{q}_l \end{aligned} \tag{9}$$

Identifying each term in Eqn. (9)

$$\begin{aligned} \left.\frac{\partial \mathbf{x}}{\partial \mathrm{q}_k}\right|_{\mathbf{q}=\mathbf{0}} &= \Phi_k + \sum_{p=1}^{\mathrm{r}} \left.\frac{\partial \Phi_p}{\partial \mathrm{q}_k}\right|_{\mathbf{q}=\mathbf{0}} \mathrm{q}_p \\ &= \Phi_k \\ \left.\frac{\partial^2 \mathbf{x}}{\partial \mathrm{q}_k \partial \mathrm{q}_l}\right|_{\mathbf{q}=\mathbf{0}} &= \frac{\partial \Phi_k}{\partial \mathrm{q}_l} + \frac{\partial \Phi_l}{\partial \mathrm{q}_k} + \sum_{p=1}^{\mathrm{r}} \left.\frac{\partial^2 \Phi_p}{\partial \mathrm{q}_k \partial \mathrm{q}_l}\right|_{\mathbf{q}=\mathbf{0}} \mathrm{q}_p \\ &= \frac{\partial \Phi_k}{\partial \mathrm{q}_l} + \frac{\partial \Phi_l}{\partial \mathrm{q}_k} \\ &= \partial \Phi_{kl} \end{aligned} \tag{10}$$

allows writing the solution naturally as a sum of a set of LNMs and modal derivatives.

$$\mathbf{x}(\mathbf{q}) = \begin{bmatrix} \boldsymbol{\Phi} & \partial\boldsymbol{\Phi} \end{bmatrix} \begin{bmatrix} \mathbf{q} \\ \mathbf{p} \end{bmatrix} \tag{11}$$

where $\mathbf{p}$ refers to the unified variables $\mathrm{q}_k\mathrm{q}_l$ associated with the MDs.

The computation of the MDs can be performed in several ways [16]. Analytic formulas are proposed which take the mass into account or not and they are well-suited for simple problems where the jacobian of the nonlinear terms is known. A numerical solution is also proposed that relies on a finite difference method between two eigenvalue problems (Eqn. (12)): the LNMs of the structure around an equilibrium position $\boldsymbol{\Phi}$, $\mathbf{x} = \mathbf{0}$ in our case, which is not necessarily a stable equilibrium position; and the LNMs of the structure deformed along one of the previous LNMs $\boldsymbol{\Lambda}(\Phi_{\mathrm{k}})$ and which take into account the nonlinear effects, i.e. computed using the tangent stiffness.

$$\frac{\partial \Phi_k}{\partial \mathrm{q}_l} = \frac{\Phi_k - \Lambda_k(\delta h_l\, \Phi_l)}{\delta h_l} \tag{12}$$

This method is particularly well-adapted to the computation of MDs using a commercial FE solver.

2.2.3 Projection of the nonlinear forces onto the basis : STEP procedure

The projection of the nonlinear forces can be time-consuming as it is necessary to re-build the solution vector, construct the nonlinear terms and then project them onto the reduction basis. One solution is to estimate the reduced stiffnesses associated with the projection basis *a priori*, and compute the nonlinear forces directly as proposed by the STiffness Evaluation Procedure (STEP) [13].

Integrating the Green-Lagrange tensor in the FE method [20] leads to formulating the nonlinear internal forces as a third degree polynomial

$$\mathbf{f}_p^{\text{tot}}(\mathbf{x}) = \sum_{k=1}^{\text{n}} \text{K}_{pk}\,\text{x}_k + \sum_{k=1}^{\text{n}}\sum_{l=k}^{\text{n}} \text{K}^{\text{q}}_{pkl}\,\text{x}_k\,\text{x}_l + \sum_{k=1}^{\text{n}}\sum_{l=k}^{\text{n}}\sum_{m=l}^{\text{n}} \text{K}^{\text{c}}_{pklm}\,\text{x}_k\,\text{x}_l\,\text{x}_m \tag{13}$$

where $\mathbf{K}^{\,\text{q}}$ and $\mathbf{K}^{\,\text{c}}$ indicate the quadratic and cubic stiffness matrices. Projecting Eqn. (13) onto the basis $\mathbf{\Phi}$ leads to the reduced internal forces

$$\begin{aligned}\mathbf{f}^{\text{tot}}_{\text{red},p}(\mathbf{x}) &= \Phi_p^\intercal\,\mathbf{f}^{\text{tot}}(\mathbf{\Phi}\,\mathbf{q}) \\ &= \sum_{k=1}^{\text{r}} \beta_{pk}\,\text{q}_k + \sum_{k=1}^{\text{r}}\sum_{l=k}^{\text{r}} \beta^{\text{q}}_{pkl}\,\text{q}_k\,\text{q}_l + \sum_{k=1}^{\text{r}}\sum_{l=k}^{\text{r}}\sum_{m=l}^{\text{r}} \beta^{\text{c}}_{pklm}\,\text{q}_k\,\text{q}_l\,\text{q}_m\end{aligned} \tag{14}$$

where $\boldsymbol{\beta}$, $\boldsymbol{\beta}^{\,\text{q}}$ and $\boldsymbol{\beta}^{\,\text{c}}$ are the reduced linear, quadratic and cubic stiffness matrices. The method proposed by Muravyov [13] allows determining the reduced stiffnesses through several static loads along linear combinations of vectors of the basis. For example, to compute the terms of the form β_{pi}, β^{q}_{pii} and β^{c}_{piii}, at least three loadings are required along the vector Φ_i at different amplitudes, providing the necessary equations (Eqn. (15)). Note that $\boldsymbol{\beta}$ can be obtained simply by projecting the linear stiffness $\mathbf{K}$ onto the basis $\mathbf{\Phi}$. Similarly, $\beta^{\text{q}}_{\text{pij}}$, $\beta^{\text{c}}_{\text{pijj}}$ and β^{c}_{piij} are obtained through loadings along $h_i\Phi_i + h_j\Phi_j$ with differents h_i and h_j (Eqn. (16)), and β^{c}_{pijk} with $h_i\Phi_i + h_j\Phi_j + h_k\Phi_k$ (Eqn. (17)). In all the cases $i \leqslant j \leqslant k$.

$$\begin{aligned}\mathbf{f}^{\text{tot}}_{\text{red},p}(h_i\Phi_i) &= \Phi_p^\intercal\mathbf{f}^{\text{tot}}(h_i\Phi_i) \\ &= \beta_{pi}\,h_i + \beta^{\text{q}}_{pii}\,h_i^2 + \beta^{\text{c}}_{piii}\,h_i^3\end{aligned} \tag{15}$$

$$\begin{aligned}\Phi_p^\intercal\,\mathbf{f}^{\text{tot}}(h_i\Phi_i + h_j\Phi_j) = {}& \beta_{pi}h_i + \beta^{\text{q}}_{pii}\,h_i^2 + \beta^{\text{c}}_{piii}h_i^3 \\ &+ \beta_{pj}h_j + \beta^{\text{q}}_{pjj}h_j^2 + \beta^{\text{c}}_{pjjj}h_j^3 \\ &+ \beta^{\text{q}}_{pij}h_ih_j + \beta^{\text{c}}_{piij}h_i^2h_j + \beta^{\text{c}}_{pijj}h_ih_j^2\end{aligned} \tag{16}$$

$$\begin{aligned}\Phi_p^\intercal\mathbf{f}^{\text{tot}}(h_i\Phi_i + h_j\Phi_j + h_k\Phi_k) = {}& \beta_{pi}h_i + \beta^{\text{q}}_{pii}h_i^2 + \beta^{\text{c}}_{piii}h_i^3 \\ &+ \beta_{pj}h_j + \beta^{\text{q}}_{pjj}h_j^2 + \beta^{\text{c}}_{pjjj}h_j^3 \\ &+ \beta_{pk}h_k + \beta^{\text{q}}_{pkk}h_k^2 + \beta^{\text{c}}_{pkkk}h_k^3 \\ &+ \beta^{\text{q}}_{pij}h_ih_j + \beta^{\text{c}}_{piij}h_i^2h_j + \beta^{\text{c}}_{pijj}h_ih_j^2 \\ &+ \beta^{\text{q}}_{pik}h_ih_k + \beta^{\text{c}}_{piik}h_i^2h_k + \beta^{\text{c}}_{pikk}h_ih_k^2 \\ &+ \beta^{\text{q}}_{pjk}h_jh_k + \beta^{\text{c}}_{pjjk}h_j^2h_k + \beta^{\text{c}}_{pjkk}h_jh_k^2 \\ &+ \beta^{\text{c}}_{pijk}h_ih_jh_k\end{aligned} \tag{17}$$

Table 1: Properties of the reference sector

$\mathbf{L}_c$	$\mathbf{w}_c$	$\mathbf{t}_c$	$\mathbf{N}_c$	$\mathbf{L}_{bl}$	$\mathbf{w}_{bl}$	$\mathbf{t}_{bl}$	$\mathbf{N}_{bl}$	k
0.1 m	0.02 m	0.01 m	6	0.1 m	0.02 m	0.002 m	30	$1e5\,\mathrm{N.m}^{-1}$

3 Frequency Analysis: the Harmonic Balance Method (HBM)

The complete and reduced solutions of Eqn. (1) are studied in the framework of a frequency analysis. Their limit cycles are searched by assuming a solution of the form

$$\mathbf{x}(t) = \mathbf{a}_0 + \sum_{k=1}^{N_h} \left(\mathbf{a}_k \cos(k\omega t) + \mathbf{b}_k \sin(k\omega t)\right) \tag{18}$$

Substituting Eqn. (18) in the general equation, complete Eqn. (1) or reduced Eqn. (7), and projecting it onto the basis of the harmonic function with respect to the adapted scalar product

$$\langle f(t), g(t)\rangle = \frac{\omega}{\pi}\int_0^{\frac{2\pi}{\omega}} f(t)\, g(t)\, \mathrm{d}t \tag{19}$$

leads to the general equation of the HBM

$$\mathbf{Z}(\omega)\,\widehat{\mathbf{x}} + \widehat{\mathbf{f}}^{\,\mathrm{nl}}(\widehat{\mathbf{x}}) = \widehat{\mathbf{f}}^{\,\mathrm{ext}} \tag{20}$$

where $\widehat{\mathbf{x}}$, $\widehat{\mathbf{f}}^{\,\mathrm{nl}}$ and $\widehat{\mathbf{f}}^{\,\mathrm{ext}}$ are the Fourier coefficients of $\mathbf{x}$, $\mathbf{f}^{\,\mathrm{nl}}$ and $\mathbf{f}^{\,\mathrm{ext}}$, while $\mathbf{Z}$ is the dynamic stiffness expressed as

$$\mathbf{Z} = \begin{bmatrix} 2\mathbf{K} & & \\ & \mathbf{Z}_1 & \\ & & \ddots \\ & & & \mathbf{Z}_{N_h} \end{bmatrix}, \; \mathbf{Z}_k = \begin{bmatrix} \mathbf{K} - (k\omega)^2\mathbf{M} & k\omega\mathbf{C} \\ -k\omega\mathbf{C} & \mathbf{K} - (k\omega)^2\mathbf{M} \end{bmatrix} \tag{21}$$

The Fourier coefficients of the nonlinear terms are not easily computable analytically, except for very simple systems. Thus, an Alternating Frequency-Time (AFT) method [2] is used to determine them as it allows computing nonlinear terms regardless of the nonlinearity involved. The method consists in passing forwards and backwards in the frequency and time domains using direct ($\mathbf{F}$) and inverse ($\overline{\mathbf{F}}$) discrete Fourier transformation matrices. A flow chart of the method is presented in (Fig. 1).

4 Application

4.1 Presentation of the model

The structure considered for the application of the method proposed is a schematic stator vane composed of 6 blades ($\bullet_{bl}$) and 2 rings ($\bullet_c$) providing the coupling between the blades (Fig. 2a). A beam model is proposed Fig. 2b, and the repeating sector is shown in Fig. 2c. The dimensions of the beams representing the blades and the rings are given in (Tab. 1) (Length, width, thickness), and the finite element discretization in (Fig. 2d, Tab. 1). The springs can be assimilated with locating pins used to fix the vane on the carter. Thus, the complete model is composed of 726 DOFs.

4.1.1 Nonlinear Euler-Bernoulli theory

The beams are modelled using a classical Euler-Bernoulli theory, with u being the longitudinal displacement, v the transversal displacement and θ the rotation of the sections.

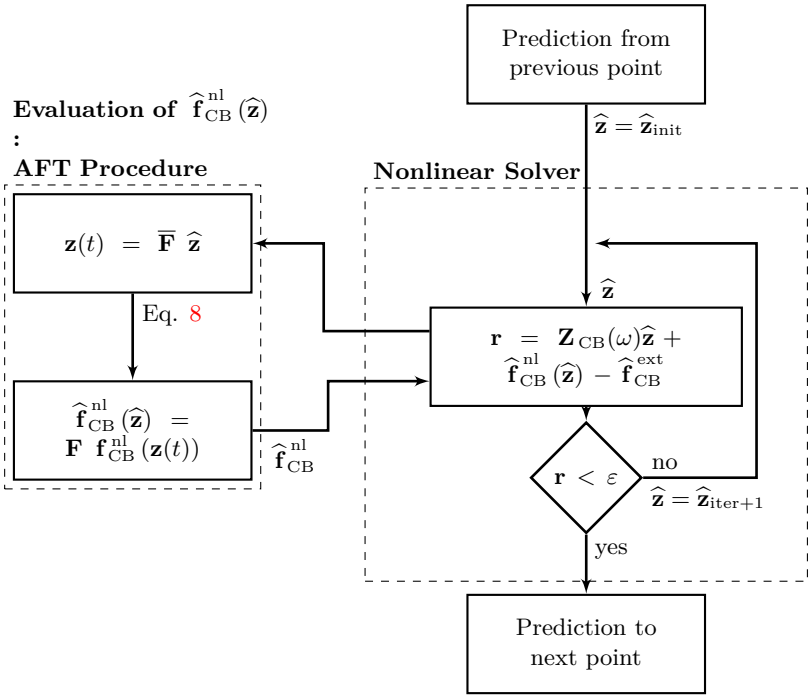

Fig. 1: HBM procedure of the reduced system

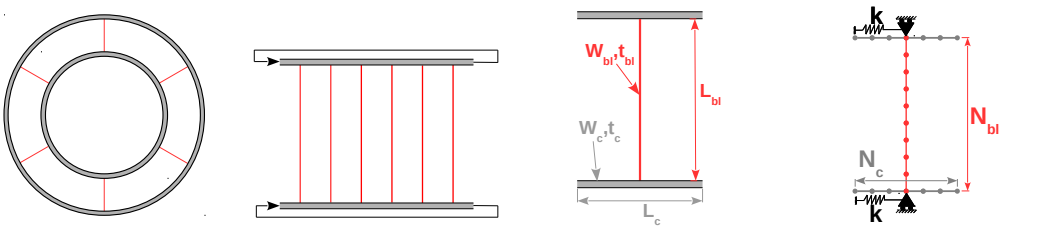

(a) cyclic symmetric model (b) beam representation (c) dimensions of the reference sector (d) finite element representation of the reference sector

Fig. 2: Stator vane model

The general displacements are thus expressed as

$$\mathbf{u}(x,y) = \begin{bmatrix} u(x) - y\,\theta(x) \\ v(x) \end{bmatrix} \tag{22}$$

The nonlinearities are a consequence of the large strains of the beam, which leads to considering the nonlinear part of the Green tensor.

$$\boldsymbol{\epsilon} = \frac{1}{2}\left(\nabla\mathbf{u} + \nabla^{\intercal}\mathbf{u}\right) + \frac{1}{2}\nabla\mathbf{u}\,\nabla^{\intercal}\mathbf{u} \tag{23}$$

The constraint along the longitudinal displacement of the model allows applying the von Kàrmàn hypothesis [18] and simplifying Eqn. (23)

$$\begin{aligned} \boldsymbol{\epsilon} &= \epsilon_{xx} \\ &= u_{,x} - y\,v_{,xx} + \frac{1}{2}v_{,x}^2 \end{aligned} \tag{24}$$

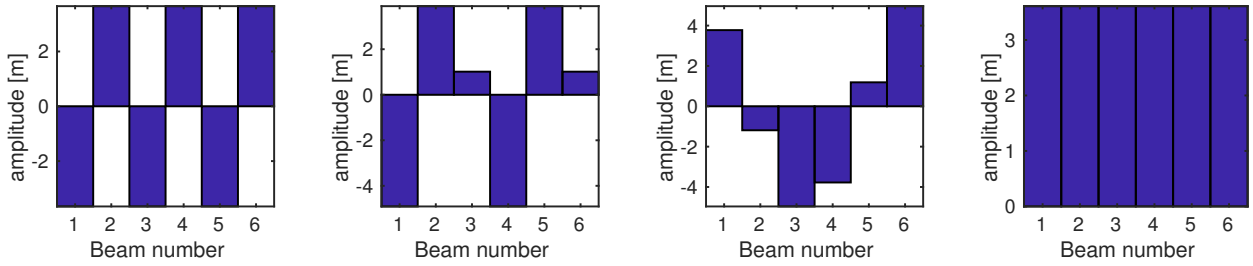

(a) 3 Diameters (b) 2 Diameters (c) 1 Diameter (d) 0 Diameter

Fig. 3: Mode shapes of the first flexural mode family

Table 2: Pulsations of the first flexural mode family

Nodal diameters	3	2	1	0
Pulsation [rad/s]	6638	6662.3	6676.7	6907.4

Using Eqn. (24) in the strain energy

$$\mathrm{E_p} = \frac{1}{2}\int_0^{\mathrm{L}} \left(\mathrm{ES}\left(u_{,x}^2 + u_{,x}\, v_{,x}^2 + \frac{1}{4} v_{,x}^4 \right) + \mathrm{EI}\, v_{,xx}^2 \right) \mathrm{d}x \tag{25}$$

where $\mathrm{S} = \mathrm{w} \times \mathrm{t}$ and $\mathrm{I} = \dfrac{\mathrm{w} \times \mathrm{t}^3}{12}$, and applying Lagrange's equations gives the linear and nonlinear stiffness matrices. The linear mass matrices are determined thanks to the kinetic energy. The material used is a classical steel ($\mathrm{E} = 210\,\mathrm{GPa}$, $\rho = 7800\,\mathrm{kg/m}^3$).

4.2 Study of the underlying linear system

4.2.1 Complete system

Let us consider the system described by Eqn. (2). In the case of cyclic symmetry, the system will be subject to simple and double eigenvalues, characterized by nodal diameter mode shapes [15]. This study focuses on the first flexural mode family of the blades. The mode shapes are represented in Fig. 3, where the amplitude is taken at the middle of each beam transversally. Classical results are obtained, with 0 and 3 diameters (as there are 6 sectors) as simple modes and 1 and 2 diameters as double modes.

The forced response of the system is computed in order to account for all the diameters. Thus, the excitation is applied at the middle of one of the beams transversally. The excited beam is numbered 1, the other following beams are numbered consecutively. A Rayleigh damping is applied that takes into account the mass matrix and a damping ratio of 0.1% on the 3 diameter modes. The result is plotted in Fig. 4. The graph represents the transversal amplitude at the middle of each beam.

The 0 diameter mode is clearly identified with all the beams having the same amplitude ($\omega \approx 6900\,\mathrm{rad/s}$). The other diameter modes, especially the 3 diameters (1^{st} peak), do not appear so clearly, certainly due to the proximity of those 3 modes.

4.2.2 Linear Craig & Bampton reduction

As the simulations are conducted for the first flexural mode family, the reduction of each substructure is performed with the first flexural mode $\Phi_{1\mathrm{F}}$. In order to process the nonlinearities in the followings parts, a modal derivative is added to the LNM. To simulate a simple system like a beam, the modal derivative $\partial\Phi_{11}$ is sufficient, in addition to the LNM, to take the nonlinear effects into account [6]. Therefore the basis for the internal modes of the substructures is $\Phi_{\mathrm{i}} = \left[\Phi_{1\mathrm{F}}\ \partial\Phi_{11}\right]$. The reduction allows reducing the number of unknowns from 726 to 48 (6×2 internal modes plus 2×3 statics modes for each of the 6 junctions between substructures), equivalent to 93.4 %. The modal derivative $\partial\Phi_{11}$ was computed with $\delta h = 1e^{-3}$ (Eqn. (12)).

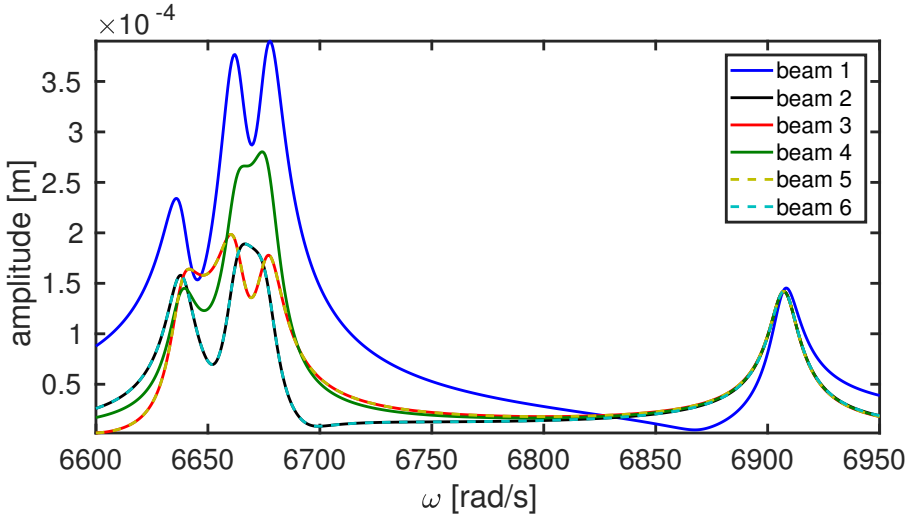

Fig. 4: Linear forced response of the system for F=1N

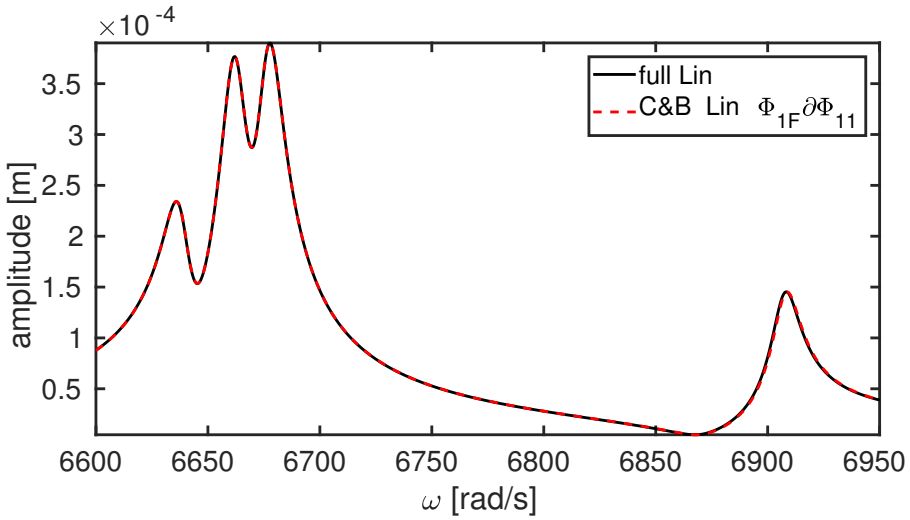

Fig. 5: Comparison of the results obtained with reduction on beam 1

Table 3: Error on the linear reduction

Nodal diameters	3	2	1	0
Reference puls. [rad/s]	6638	6662.3	6676.7	6907.4
Reduced puls. [rad/s]	6638.1	6662.3	6676.7	6907.9
Relative error [%]	$5.4e^{-4}$	$1.4e^{-4}$	$1.7e^{-5}$	$6.6e^{-3}$

The results of the linear reduction (Fig. 5 and Tab. 3) show good correlation with the complete model with less than $7e^{-3}$% error on the frequencies. Thus, as this basis shows its reliability in the linear context, it will be used again in the nonlinear reduction procedure.

4.3 Simulation of the full nonlinear system

Let us assume that only the thin blades are subjected to nonlinearities. As the rings are thick compared to the blades, they do not undergo such effects.

The solutions presented in Fig. 6 are computed on the full system with respect to the HBM. The solutions for 3

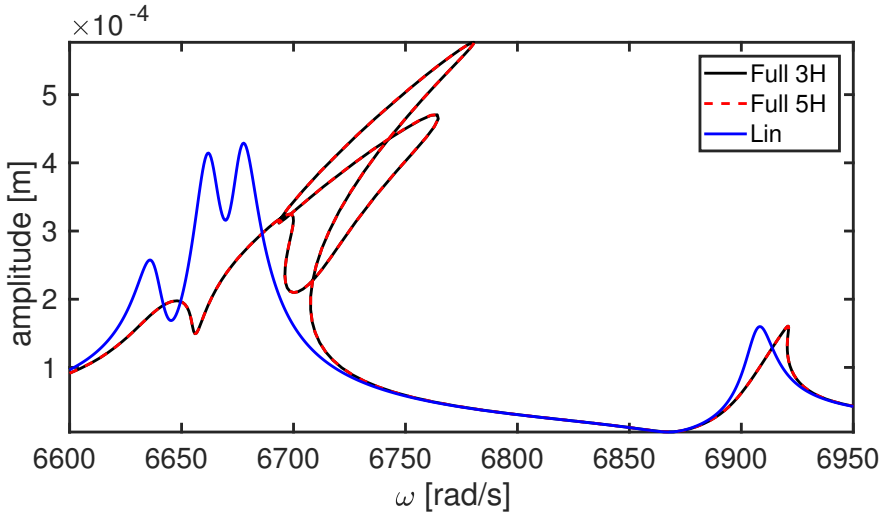

Fig. 6: Comparison of the results obtained with 3 and 5 harmonics in the HBM on the beam 1 with F=1.1N

and 5 harmonics are compared and they are perfectly superposed, the 3 harmonics solution can thus be considered as harmonically converged. In the following, the solutions presented will be computed with 3 harmonics.

In order to present the global results, the following outcomes are plotted in a pulsation-energy diagram [4, 5] such that

$$E(\mathbf{x}) = \sqrt{\|\mathbf{a}_0\|^2 + \sum_{k=0}^{\mathrm{N_h}} \left(\|\mathbf{a}_k\|^2 + \|\mathbf{b}_k\|^2 \right)} \tag{26}$$

An example is given in Fig. 7 with responses of the system to several excitations.

As the amplitude of excitation increases, the nonlinearity becomes increasingly visible (Fig. 7). From F=0.6N, the system seems to follow a bifurcated branch, like those preesented by Grolet [5]. The time series in Fig. 8b–8c, representing the transversal amplitude at the middle of each beam as a function of time, clearly highlights that the amplitude is mostly localized on the excited beam, number 1, in the nonlinear case (Fig. 8b), whereas the linear time response is similar to the 1 diameter linear mode (Fig. 8c). In addition, still referring to the time series (Fig. 8b), beam 1 is in phase opposition with all the other beams, which totally breaks the nodal diameter characteristic of the mode (Fig. 3c). In the following, the time series will be taken at the resonance peak of the 1 diameter mode, for both linear and nonlinear signals.

The behaviours in play demonstrate the usefulness of the study and the need to perform it within an acceptable time. Although the analysis is performed along a simplified structure, the phenomena exhibited appear at moderate amplitudes and highlight a strong localisation on the beam 1, clearly showing the limitations of the linear approach and the risks subjected by the structure.

4.4 Reduction of the model

The basis presented in the linear study is re-utilized for the reduction of the nonlinear system. The whole nonlinear procedure presented previously is applied, and the nonlinear terms of each substructure are projected using the STEP procedure on the basis and then assembled along the boundary DOFs. The reduced stiffnesses are computed with $h_i = 1e^{-3}$ and $h_j = 5e^{-3}$ (Eqns. (15–16)) (2 coefficients are needed as there are 2 vectors in the basis). The results of the simulations can be seen in Fig. 9 and the correlation between the full and the reduced models is quite good, whether for the bifurcated diameter mode or the unbifurcated ones (Figs. 9a). The behaviour of the structure around the bifurcation is also well reproduced (Figs. 9b–9c) compared to the full nonlinear response. The computation times are presented in Tab. (4) and demonstrate a significant gain thanks to the reduction, more than 99 %. It is noteworthy that the whole offline computation, including the computation of the linear mode, the modal derivative and the STEP coefficients, lasts less than 0.2 s.

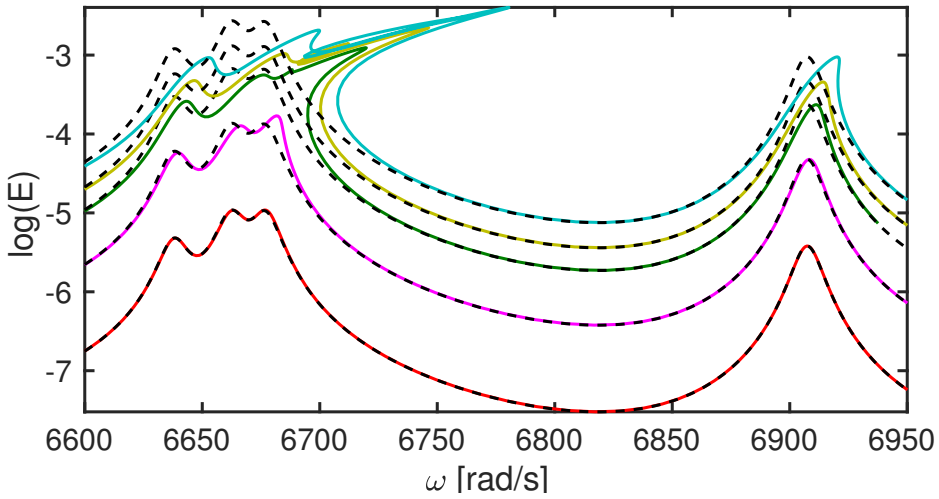

Fig. 7: Pulsation-Energy diagram of the full nonlinear system for several forcing amplitudes (Linear: **- -**, Nonlinear: **0.1N**, **0.3N**, **0.6N**, **0.8N**, **1.1N**)

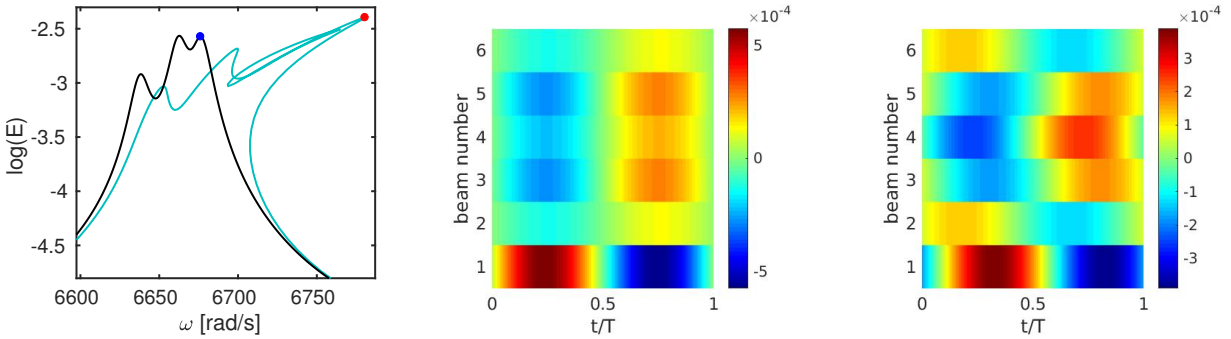

(a) Forced responses associated with the frequency range of interest

(b) Nonlinear time evolution of the transversal DOF at the middle of each beam (•)

(c) Linear time evolution of the transversal DOF at the middle of each beam (•)

Fig. 8: Highlighting the localization on the 1 diameter mode for F=1.1N

Table 4: Gain in time of the reduction

F [N]	Full [s]	Reduced [s]	Gain in time [%]
0.6	11927	89.97	99.246
0.8	9264	44.4	99.5
1.1	10243	73.2	99.286

4.5 Parametric study: impact of the rings

Thanks to the capacities of the method, a parametric study is performed on the thickness of the rings. The thickness was chosen in the range $[-40\%\ +40\%]$ of the initial model. The results in terms of forced responses and time series of the 1 diameter mode are visible in Fig. 10.

The first impact of the rings' thickness on the structure is observable on the linear frequencies of the diameter modes. Indeed, the thinner the rings are, the farther the frequencies are from each other due to the strength of the coupling performed by the rings.

This also has a clear impact on the nonlinear response of the system. For a weak coupling, i.e. $\mathbf{t}_c = 0.6\,\text{cm}$, the system appears to show no bifurcation, as highlighted in Fig. 10a. This is supported by the time series in Fig. 10b where the 1 diameter mode appears clearly. For stronger coupling, $\mathbf{t}_c > 0.6\,\text{cm}$, the 1 diameter mode

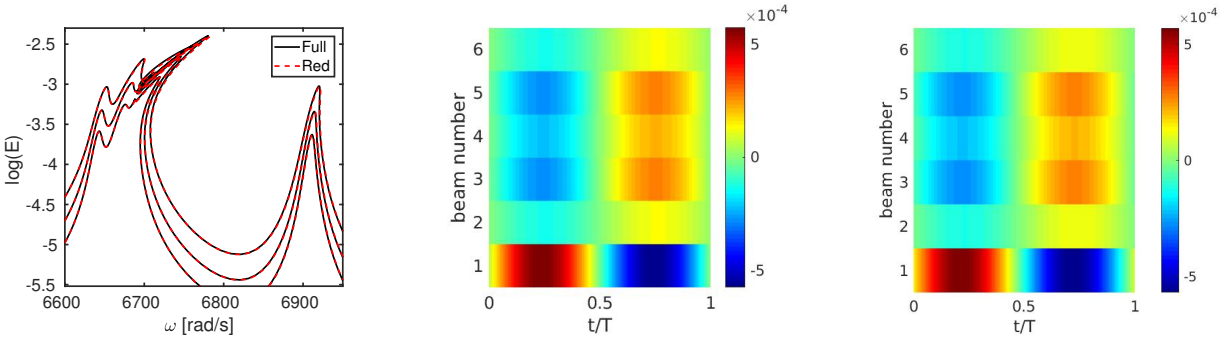

(a) Forced responses of the system

(b) Nonlinear time evolution of the transversal DOF at the middle of each beam: full nonlinear system F=0.6N

(c) Nonlinear time evolution of the transversal DOF at the middle of each beam: reduced nonlinear system F=0.6N

Fig. 9: Comparison of the full and reduced models

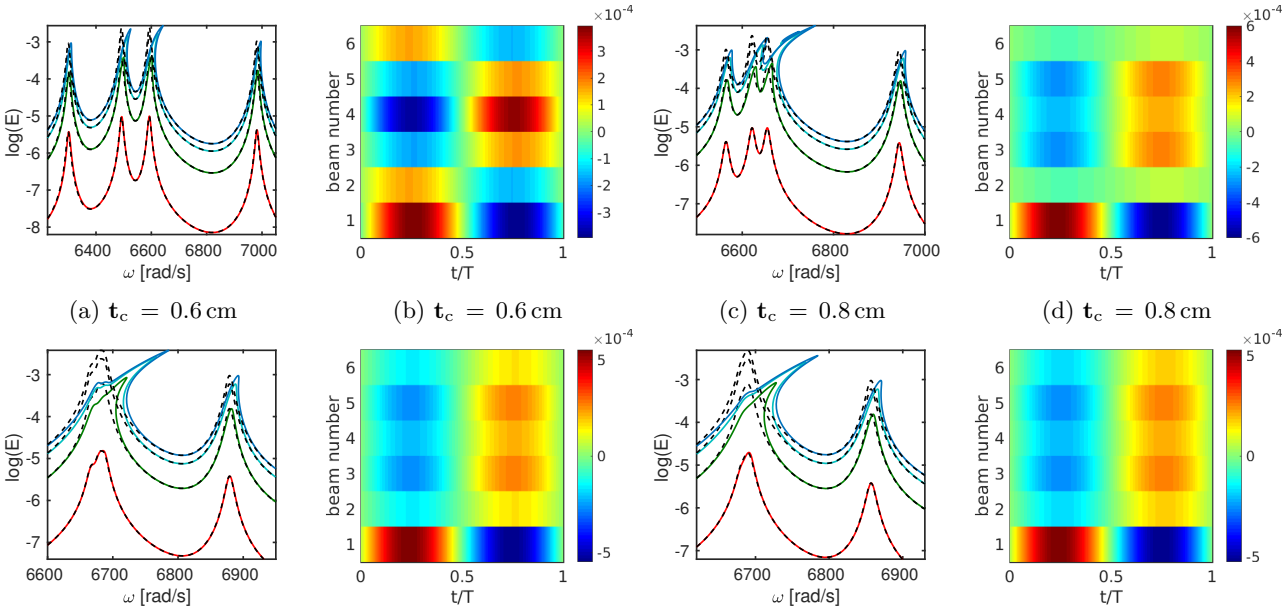

(a) $\mathbf{t}_c = 0.6\,\text{cm}$ (b) $\mathbf{t}_c = 0.6\,\text{cm}$ (c) $\mathbf{t}_c = 0.8\,\text{cm}$ (d) $\mathbf{t}_c = 0.8\,\text{cm}$

(e) $\mathbf{t}_c = 1.2\,\text{cm}$ (f) $\mathbf{t}_c = 1.2\,\text{cm}$ (g) $\mathbf{t}_c = 1.4\,\text{cm}$ (h) $\mathbf{t}_c = 1.4\,\text{cm}$

Fig. 10: Influence of the thickness of the rings (Linear: **- -**, Nonlinear: **0.1N**, **0.5N**, **0.8N**, **1.1N**)

reaches the bifurcated branch, as shown in Figs. 10c–10e–10g and the phase opposition of the beam 1 with the others (Figs. 10d–10f–10h). For approximately the same energy level, the bifurcation of the 1 diameter mode is thus expected to occur for a coupling thickness between 0.6 cm and 0.8 cm.

The time series Figs. 10b–10d–10f–10h also leads to a configuration where the amplitude localization is particularly marked for $\mathbf{t}_c = 0.8\,\text{cm}$. In this case, the risk of reaching the fatigue limit is more significant than the others, highlighting the impact that such nonlinear localization phenomena can have on the design process.

5 Conclusion

This work was devoted to the presentation of a reduction procedure suited to the study of structures subjected to geometric nonlinearities. The method is based on a component mode synthesis, completed by the use of modal derivatives and a stiffness evaluation procedure in order to reduce the nonlinear terms. The application was tested on a schematic stator vane composed of nonlinear beams. The results showed that the procedure is efficient in taking into account the nonlinear behaviours of the structure, especially the specific dynamical effects associated with cyclic symmetry such as energy localization. What is more it provides an interesting gain in time.

Besides the reduction procedure, this paper illustrated the extreme behaviours that a cyclic system can be

exposed to. The nonlinear effects exhibited strong localizations on the structure at low amplitudes which must be avoided to ensure the integrity of the components. The method proposed here allowed performing this study in accordance with the imperative of reducing design time, for example, with respect to the thickness of the rings, and highlighting the presence or not of localization and its significance.

In further works, it would be interesting to perform such a study with NNMs and compare it with the results of the forced responses presented in this paper. This would allow predicting the bifurcation points more easily in a design procedure. Also, the extension of the method to a more realistic and complex system, such as a 3D bladed disk, is planned to assess its real potential. Lastly, coupling this method with that proposed by Joannin [8] to incorporate friction non-linearity in the model will also be considered.

Nomenclature

NNM	Nonlinear Normal Mode.
FE	Finite Element.
CMS	Component Mode Synthesis.
LNM	Linear Normal Mode.
MD	Modal Derivative.
STEP	STiffness Evaluation Procedure.
DOF	Degree Of Freedom.
AFT	Alternating Frequency-Time.
HBM	Harmonic Balance Method.
$\mathbf{x}(\mathrm{t})$	Vector of unknowns in the physical coordinates.
$\mathbf{y}(\mathrm{t})$	Vector of unknowns ordered along the internal and boundary DOFs.
$\mathbf{z}(\mathrm{t})$	Vector of unknows in the reduced coordinates.
$\mathbf{f}^{\mathrm{ext}}(t)$, $\mathbf{f}^{\mathrm{nl}}(t)$	External and nonlinear forces.
$\boldsymbol{\Phi}_{\mathrm{i}}^{\mathrm{k}}$, $\boldsymbol{\Psi}_{\mathrm{b}}^{\mathrm{k}}$	Internal eigenvectors and static modes of the k^{th} sub-structure.
$\boldsymbol{\Lambda}$	LNMs of the deformed structure.
$\mathbf{a}_{\mathrm{k}}$, $\mathbf{b}_{\mathrm{k}}$	Fourier coefficients of the solution.
$\widehat{\bullet}$	Vector of Fourier coefficients.
$\mathbf{M}$, $\mathbf{C}$, $\mathbf{K}$	Mass, damping and linear stiffness matrices.
$\mathbf{T}_{\mathrm{CB}}$	Transformation matrix of the Craig-Bampton Method
$\mathbf{K}^{\mathrm{q}}$, $\mathbf{K}^{\mathrm{c}}$	Quadratic and cubic stiffness matrices.
$\boldsymbol{\beta}$, $\boldsymbol{\beta}^{\mathrm{q}}$, $\boldsymbol{\beta}^{\mathrm{c}}$	Linear, quadratic and cubic reduced stiffness matrices.
$\mathbf{Z}$	Dynamic stiffness matrice.
$\boldsymbol{\epsilon}$	Green-Lagrange tensor.
$\mathrm{N_S}$	Number of sectors.
$\mathrm{N_h}$	Number of harmonics.
ω	Excitation pulsation.
L, w, t	Length, width and thickness of the beams.
$\mathrm{N_c}$, $\mathrm{N_{bl}}$	Number of elements in the FE model.
u, v, θ	Displacements in the Euler-Bernoulli formulation.
E, S, I, ρ	Young's modulus, section, moment of inertia and density.
$\bullet_{\mathrm{i}}$, $\bullet_{\mathrm{b}}$	Subscripts associated with internal and boundary values.
$\bullet_{\mathrm{c}}$, $\bullet_{\mathrm{bl}}$	Subscripts associated with ring and blade values.
$\bullet_{,x}$	Differentiation with respect to variable x.
∇	Nabla differential operator.

References

[1] P. Apiwattanalunggarn, S. W. Shaw, and C. Pierre. Component mode synthesis using nonlinear normal modes. *Nonlinear Dynamics*, 41(1):17–46, Aug 2005.

[2] T. M. Cameron and J. Griffin. An Alternating Frequency/Time Domain Method for Calculating the Steady-State Response of Nonlinear Dynamic Systems. *Journal of Applied Mechanics*, 1989.

[3] R. R. Craig and M. C. C. Bampton. Coupling of Substructures for Dynamic Analyses. *AIAA Journal*, 6(7):1313–1319, 1968.

[4] F. Georgiades, M. Peeters, G. Kerschen, and G. J.-C. Modal analysis of a nonlinear periodic structure with cyclic symmetry. *AIAA Journal*, 47(4):1014–1025, 2009.

[5] A. Grolet and F. Thouverez. Free and forced vibration analysis of a nonlinear system with cyclic symmetry: Application to a simplified model. *Journal of Sound and Vibration*, 331:2911âĂŞ2928, 2012.

[6] A. Grolet and F. Thouverez. Model Reduction for nonlinear vibration analysis of structural systems using modal derivatives and stiffness evaluation procedure. In *The 4th Canadian Conference on Nonlinear Solid Mechanics, CanCNSM 2013*, pages paper 731, Pages: 1–6, Montreal, Canada, July 2013.

[7] S. R. Idelsohn and A. Cardona. A reduction method for nonlinear structural dynamic analysis. *Computer Methods in Applied Mechanics and Engineering*, 49(3):253 – 279, 1985.

[8] C. Joannin, B. Chouvion, F. Thouverez, J.-P. Ousty, and M. Mbaye. A nonlinear component mode synthesis method for the computation of steady-state vibrations in non-conservative systems. *Mechanical Systems and Signal Processing*, 83:75–92, 2017.

[9] G. Kerschen, M. Peeters, J. Golinval, and A. Vakakis. Nonlinear normal modes, part i: A useful framework for the structural dynamicist. *Mechanical Systems and Signal Processing*, 23(1):170 – 194, 2009. Special Issue: Non-linear Structural Dynamics.

[10] M. Krack, L. Panning-von Scheidt, and J. Wallaschek. A method for nonlinear modal analysis and synthesis: Application to harmonically forced and self-excited mechanical systems. *Journal of Sound Vibration*, 332:6798–6814, Dec. 2013.

[11] M. Krack, L. Salles, and T. Thouverez. Vibration prediction of bladed disks coupled by friction joints. *Archives of Computational Methods in Engineering*, 24(3):589–636, jul 2016.

[12] A. Lazarus, O. Thomas, and J.-F. Deu. Finite element reduced order models for nonlinear vibrations of piezoelectric layered beams with applications to nems. *Finite Elements in Analysis and Design*, 49(1):35 – 51, 2012. Analysis and Design of MEMS/NEMS.

[13] A. A. Muravyov and S. A. Rizzi. Determination of nonlinear stiffness with application to random vibration of geometrically nonlinear structures. *Computers & Structures*, 81(15):1513 – 1523, 2003.

[14] T. Nguyen. *Non linear dynamic of coupled mechanical systems: model reduction and identification.* PhD Thesis, École Nationale des Ponts et Chaussées, 2007.

[15] S. Samaranayake, A. K. Bajaj, and O. D. I. Nwokah. Amplitude modulated dynamics and bifurcations in the resonant response of a structure with cyclic symmetry. *Acta Mechanica*, 109(1):101–125, Mar 1995.

[16] P. Slaats, J. de Jongh, and A. Sauren. Model reduction tools for nonlinear structural dynamics. *Computers Structures*, 54(6):1155 – 1171, 1995.

[17] D. L. Thomas. Dynamics of rotationally periodic structures. *International Journal for Numerical Methods in Engineering*, 14(1):81–102, 1979.

[18] O. Thomas, A. Sénéchal, and J.-F. Deü. Hardening/softening behavior and reduced order modeling of nonlinear vibrations of rotating cantilever beams. *Nonlinear Dynamics*, 86(2):1293–1318, Oct 2016.

[19] A. Vakakis. Non-linear normal modes (NNMs) and their applications in vibration theory: an overview. *Mechanical Systems and Signal Processing*, 11(1):3 – 22, 1997.

[20] O. Zienkiewicz, R. Taylor, and J. Zhu. 5 - geometrically non-linear problems âĂŤ finite deformation. In O. Zienkiewicz, R. Taylor, and J. Zhu, editors, *The Finite Element Method Set (Sixth Edition)*, pages 127 – 157. Butterworth-Heinemann, Oxford, sixth edition edition, 2005.